Nuclear Materials and Energy 45 (2025) 102034

Contents lists available at ScienceDirect

Nuclear Materials and Energy

journal homepage: www.elsevier.com/locate/nme

Tensile properties of EUROFER97-3 after neutron irradiation at 330 °C and 540 °C to damage doses of 19–23 dpa

Vladimir Chakin *, Carsten Bonnekoh, Ramil Gaisin, Rainer Ziegler, Michael Duerrschnabel, Michael Klimenkov, Bronislava Gorr, Michael Rieth

Karlsruhe Institute of Technology (KIT), Institute for Applied Materials, P.O. Box 3640, 76021 Karlsruhe, Germany

ARTICLE INFO

Keywords:
RAFM EUROFER97-3 steel
Radiation hardening and embrittlement
Neutron irradiation

ABSTRACT

The reduced activation ferritic-martensitic (RAFM) EUROFER97-3 steel of two heat treatments (EUROFER97-3_1100/700 and EUROFER97-3_980/780) after irradiation in the BOR-60 fast reactor at temperatures of 330 °C and 540 °C, with damage doses ranging from 19.2 to 23.3 dpa exhibited fundamentally different changes in tensile properties depending on the irradiation temperature, regardless of the heat treatment used. Significant radiation hardening and embrittlement were observed after irradiation at 330 °C. In contrast, irradiation at 540 °C resulted in only minor alterations to the tensile properties compared to the unirradiated reference state. These changes can be attributed to the formation of radiation-induced defects and fine precipitates, as well as an evolution in the original phase structure.

1. Introduction

EUROFER97 steel is the result of many years of research in the development of reduced activation ferritic-martensitic (RAFM) steels for fusion applications [1,2]. Currently, the RAFM EUROFER97 steel, which was developed at KIT (formerly FZK) in Germany, is expected to serve as a primary structural material for DEMO breeding blankets [3–5]. The third batch of EUROFER97 [6], produced under the Test Blanket Module (TBM) program and referred to as EUROFER97-3, is studied in this paper.

According to the DEMO R&D program [1–5], critical properties of EUROFER97-3, including fracture mechanics (FM), tensile, Charpy impact, low-cycle fatigue (LCF), and creep data, are planned to be evaluated through neutron irradiation tests conducted in the BOR-60 fast reactor, followed by post-irradiation examinations (PIEs). The BOR-60 material testing fast reactor provides high fast neutrons fluxes, enabling damage doses of 20 dpa and 40–50 dpa to be achieved for the starter and second DEMO blankets, respectively, within reasonable irradiation periods of 2 and 4 years [7]. The irradiation temperatures of 325 °C and 550 °C serve as the lower and upper limits for both the HCPB (Helium-Cooled Pebble Bed) and WCLL (Water-Cooled Lithium Lead) blanket designs.

The objective of this paper is to investigate the tensile properties of EUROFER97-3 steel after neutron irradiation at target temperatures of 325 ± 10 °C and 550 ± 20 °C to a damage dose of 20 ± 2 dpa.

2. Experimental

2.1. Materials, specimens, heat treatment

The EUROFER97-3 plate, measuring 1015 × 532 × 33.3 mm, was manufactured by Saarschmiede Freiformschmiede GmbH following these production steps:

- melting in a vacuum induction furnace;
- remelting using a vacuum arc remelting furnace;
- forging into a 700 × 150 mm billet;
- removing scrap material from the top and bottom ends of the slab after forging;
- rolling into a plate using a trio rolling mill (thickness limit: ≥19 mm);
- conducting a quality heat treatment.

Fig. 1 shows EBSD maps of EUROFER97-3 obtained after two different heat treatments (see Table 1). The maps were acquired at a magnification corresponding to a 100 μm field of view. Both heat treatments produce a tempered martensitic microstructure characterized by lath and packet boundaries. However, a distinct difference in the characteristic packet size can be observed: after the 980/780 °C

* Corresponding author.
E-mail address: vladimir.chakin@kit.edu (V. Chakin).

https://doi.org/10.1016/j.nme.2025.102034
Received 10 September 2025; Received in revised form 23 November 2025; Accepted 24 November 2025
Available online 25 November 2025

Fig. 1. EBSD maps of EUROFER97-3 after different heat treatments: (a) 980/780; (b) 1100/700. Field of view is 100 μm.

Table 1
Heat treatments of the EUROFER97-3 tensile specimens.

Grade	Austenitization	Quenching	Tempering	Final cooling
EUROFER97-3_1100/700	1100 °C, 0.5 h	air	700 °C, 2 h	air
EUROFEF97-3_980/780	980 °C, 0.5 h	air	780 °C, 2 h	air

treatment, the average packet size is approximately 5.2 μm, whereas after the 1100/700 °C treatment, it increases to about 16.1 μm. The coarsening of the microstructure in the latter case results from the higher austenitization temperature. Overall, the EBSD maps confirm that both heat treatments yield a homogeneous tempered martensitic structure typical of EUROFER97 steel, with no significant crystallographic texture evident at the examined scale.

Microhardness measurements were performed using a Vickers microindenter under a load of 1 kg (HV1). The average hardness of the EUROFER97-3_980/780 material was 196–204 HV1, whereas the EUROFER97-3_1100/700 variant exhibited a significantly higher hardness of 313–317 HV1.

Tensile specimens were prepared with the rolling direction oriented

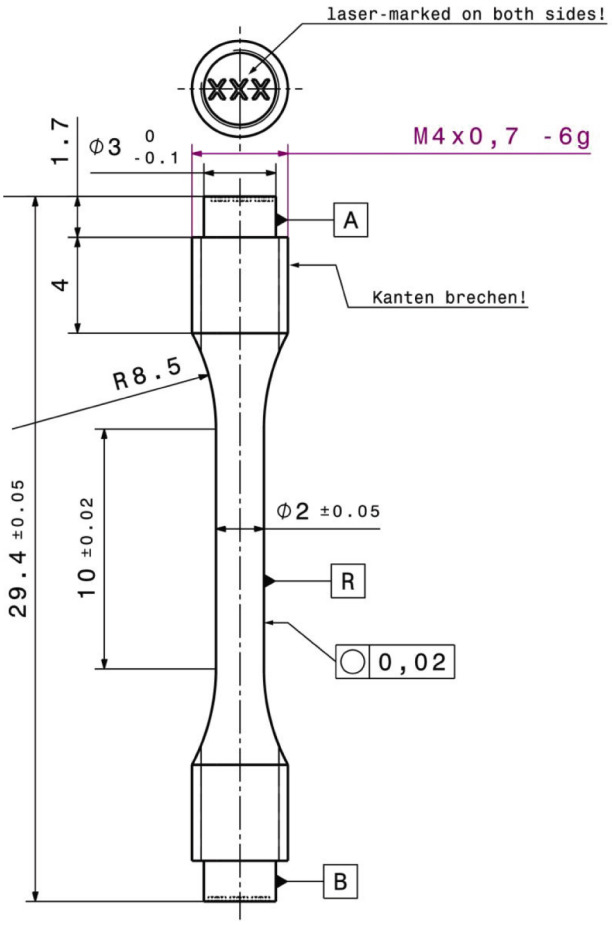

Fig. 2. Tensile specimen for irradiation testing in BOR-60 reactor.

Table 2
Chemical composition of EUROFER97-3 steel in wt.%.

Element	Specification	Analysis
Cr	8.50–9.50	9.00 ± 0.19
C	0.090–0.120	0.102 ± 0.009
N	0.015–0.045	0.0430 ± 0.0074
O	0.01	0.0004 ± 0.0001
B	0.002	0.0004 ± 0.0001
Al	0.01	0.0015 ± 0.0003
Si	0.05	0.0184 ± 0.0008
P	0.005	0.0017 ± 0.0003
Ti	0.02	0.00018 ± 0.00002
V	0.15–0.25	0.2117 ± 0.0044
Mn	0.20–0.60	0.529 ± 0.009
Fe	Not defined	87.5 ± 2.6
Co	0.01	0.0020 ± 0.0003
Ni	0.01	0.0099 ± 0.0005
Cu	0.01	0.0015 ± 0.0002
Nb	0.005	<0.0004
Mo	0.005	0.0021 ± 0.0003
Ta	0.10–0.14	0.125
W	1.00–1.20	1.152 ± 0.040

perpendicular to the specimen axis. The tensile specimens (Fig. 2), along with the creep specimens previously investigated in [8], as well as the Charpy impact, low-cycle fatigue (LCF), and other test specimens, were all machined from the EUROFER97-3 plate in two batches that differed in their heat treatment conditions (see Table 1).

The chemical composition of the EUROFER97-3 steel is shown in Table 2. The analyses were conducted at KIT (third column in Table 2), confirming good compliance with the delivery specification (second

Table 3
Irradiation parameters of IR1a and IR2 rigs in central plane of reactor core.

Rig	T_{irr}, °C target/ actual	F, $\times 10^{26}$ m^{-2}, E > 0.1 MeV	t, h	D, dpa
IR1a	325/332	5.39	12,384	24.0
IR2	550/541	5.26	11,664	23.8

Table 4
Irradiation parameters of EUROFER97-3 tensile specimens.

Grade	T_{irr}, °C target/ actual	F, $\times 10^{26}$ m^{-2}, E > 0.1 MeV	D, dpa
EUROFER97-3_1100/700	325/330	4.96	22.1
	550/540	5.15	23.3
EUROFER97-3_980/780	325/330	4.67	20.8
	550/540	4.24	19.2

column in Table 2).

2.2. Irradiation

Irradiation of EUROFER97-3 specimens was carried out in the IR1a and IR2 rigs, located in the 6th and 5th rows, respectively, of the BOR-60 fast reactor equipped with a sodium coolant. Table 3 presents the irradiation parameters for the IR1a and IR2 rigs in the central plane of the reactor core. Table 4 details the irradiation conditions for the EUROFER97-3 tensile specimens located outside the center core plane.

The specimens were placed in the perforated capsules, ensuring contact with flowing liquid sodium during irradiation. The irradiation temperatures of the specimens were calculated based on the temperature of the liquid sodium washing over them during irradiation.

The outer capsule, located in the flow of the sodium primary circuit, was made of stainless steel. The irradiation temperatures and fast neutron fluences (along with the corresponding irradiation duration, t) are presented in Table 3. These values were calculated based on known energy release data in the irradiated materials and neutron fluxes in the reactor channels. The accuracy of the temperature calculations is approximately ± 10 %, and the neutron flux estimates have an uncertainty of about ± 20 %. The damage dose was calculated for iron according to the NRT (Norgett-Robinson-Torrens) standard, based on the exact location of the tensile specimens along the height of the reactor channels used for irradiation.

Both irradiation rigs IR1a and IR2 were equipped with temperature and neutron monitors, enabling continuous monitoring of irradiation parameters. Periodic unloading of these monitors allowed their examination in a hot cell. As irradiation proceeded, new monitors were loaded into the rigs.

As shown in Table 4, both the irradiation temperatures and damage doses on the specimens remained within acceptable ranges relative to the target irradiation conditions.

2.3. Tensile testing

Testing of the EUROFER97-3 tensile specimens was conducted using the Zwick Universal Testing Machine (UTM) which was installed in a hot cell. The UTM is equipped with:

- high-temperature testing system with vacuum and a water-cooled inert gas chamber, along with a temperature controller that monitors and maintains the specimen temperature, recording temperature variations during testing;

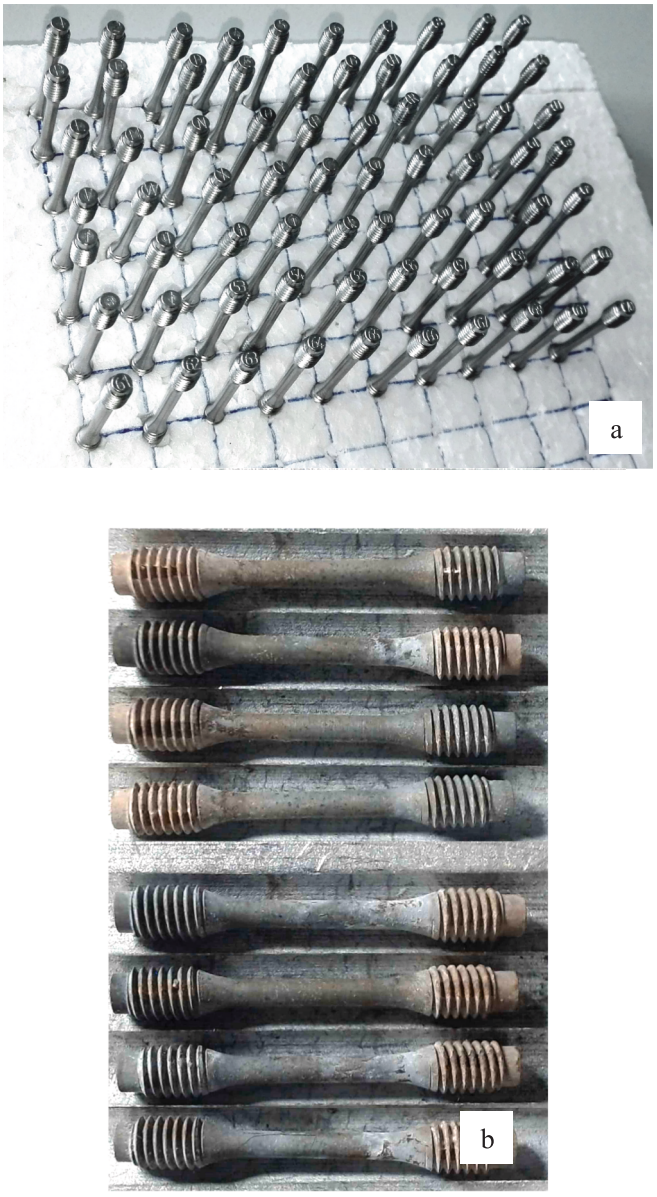

Figure 3. Appearance of EUROFER97-3 tensile specimens before (a) and after irradiation at 540 C (b)

Fig. 3. Appearance of EUROFER97-3 tensile specimens before (a) and after irradiation at 540 C (b).

- a high-temperature strain gauge (extensometer) with ceramic probe tips, enabling instrumented testing in the temperature range from room temperature to 800 °C.

The EUROFER97-3 specimens before and after irradiation were tested at a room temperature in air and at 325 °C and 550 °C in argon with the speed of testing actuator (grip) movement of 1 mm/min (strain rate 8.3×10^{-4} s^{-1}). Three specimens were tested at each test temperature however, not all tests were successful and the results of the unsuccessful tests were not included in the paper. From the load–displacement curves, strength and ductility properties including the 0.2 %-offset yield stress ($\sigma_{0.2}$), ultimate tensile strength (σ_B), uniform (ε_U) and total (ε_T) relative elongation were determined. The margin of error for strength characteristics was ± 5 %, while for relative elongation it was ± 10 %.

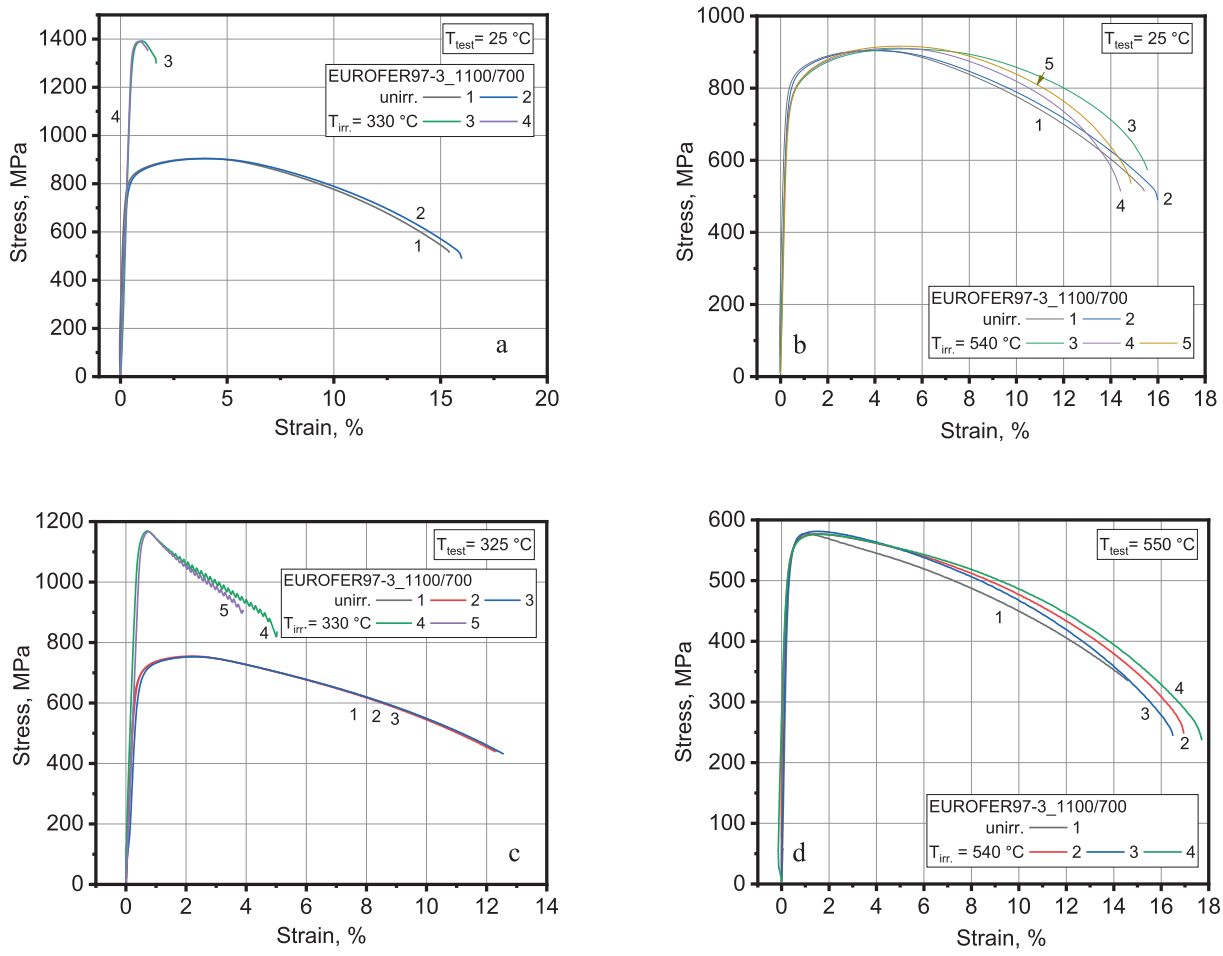

Fig. 4. Tensile stress–strain diagrams of EUROFER97-3_1100/700 after irradiation at 330 °C (a, c) and 540 °C (b, d), and testing temperatures at T_{test} = 25 °C (a, b), 325 °C (c), 550 °C (d).

3. Results

3.1. Visual inspection of EUROFER97-3 tensile specimens

The EUROFER97-3 specimens, from both heat treatments, exhibited a metallic surface luster before irradiation (see Fig. 3a).

After dismantling the IR1a and IR2 rigs at the end of the irradiation tests, the material suspensions were placed in a bath containing an aqueous ethyl alcohol solution for 6 h. This cleaning process was used to remove residual sodium from the specimen surfaces prior to disassembly in a hot cell. Once cleaning was complete, the suspensions were dried, and the specimens were carefully disassembled. The specimens then underwent additional cleaning in an ultrasonic bath with an aqueous ethyl alcohol solution, followed by drying. Visual examinations and photographs of the irradiated EUROFER97-3 specimens were performed using a Logitech C920 web camera mounted inside the hot cell.

Fig. 3b shows the appearance of the EUROFER97-3 specimens irradiated at 540 °C after the final cleaning. The specimens display minimal surface oxidation and white deposits. This is typical for steel specimens irradiated in liquid sodium, after cleaning and drying. Quantitative analysis indicates that the surface oxide layer on the irradiated specimens does not exceed 5 μm in thickness.

3.2. Tensile properties of EUROFER97-3 before and after irradiation

Fig. 4 shows the tensile stress–strain diagrams for both the unirradiated and irradiated states of EUROFER97-3_1100/700 specimens. Fig. 5 shows the corresponding diagrams for EUROFER97-3_980/780 specimens. As illustrated, the EUROFER97-3 steel with both heat treatments exhibits an excellent combination of strength and ductility before irradiation. The EUROFER97-3_1100/700 specimens demonstrate higher strength and lower ductility compared to those of the EUROFER97-3_980/780 specimens.

Irradiation at 330 °C leads to an increase in strength and a decrease in ductility for both heat treatments. Notably, the absolute strength values in the irradiated state for EUROFER97-3_1100/700 (Fig. 4a and c) are significantly higher than those for EUROFER97-3_980/780 (Fig. 5a and c). Simultaneously, the ductility sharply drops in both cases, that can be attributed to severe low-temperature radiation embrittlement (LTRE)—a well-known phenomenon characteristic of refractory body-centered cubic (bcc) metals and their alloys [9–11], as well as ferritic-martensitic steels [12–16].

Irradiation at 540 °C has a much weaker effect on the tensile properties of EUROFER97-3, regardless of the applied heat treatment (Figs. 4 and 5b and d). In this case, only a slight increase in strength is observed in the irradiated specimens, with no significant reduction in ductility.

Fig. 6 shows fragments of irradiated EUROFER97-3 specimens after tensile testing at room temperature (T_{test} = 25 °C). Although the imaging conditions inside the hot cell limit the achievable image quality, it is evident that the gauge sections of the specimens irradiated at 540 °C (Fig. 6c and d) exhibit a more elongated localized deformation zone compared to those irradiated at 330 °C (Fig. 6a and b). A comparison between EUROFER97-3_1100/700 and EUROFER97-3_980/780 (Fig. 6a and b) further reveals that the deformation localization region is more extended for EUROFER97-3_980/780 than for EUROFER97-3_1100/700. This observation is consistent with the stress–strain curves: the

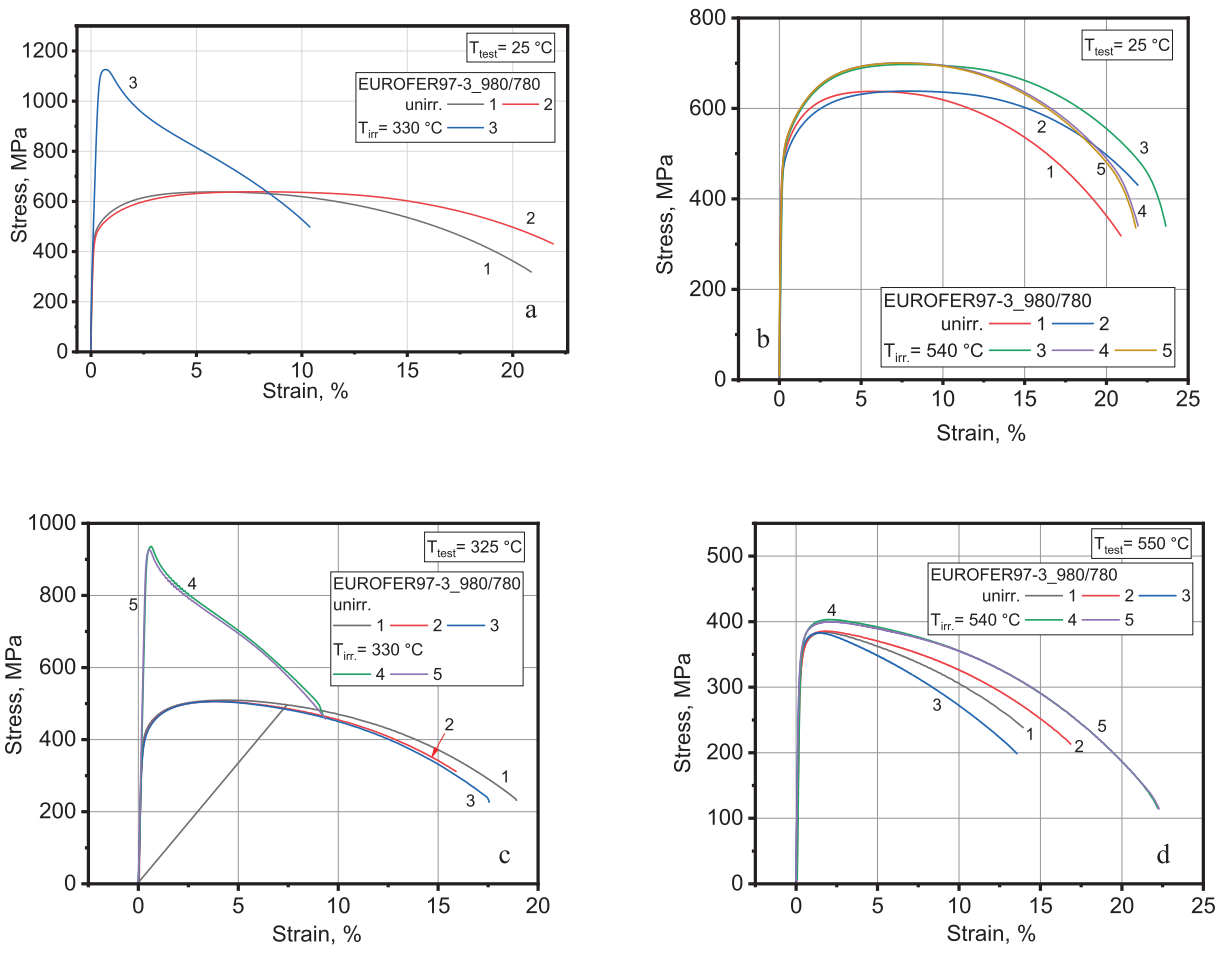

Fig. 5. Tensile stress–strain diagrams of EUROFER97-3_980/780 after irradiation at 330 °C (a, c) and 540 °C (b, d), and at testing temperatures T_{test} = 25 °C (a, b), 325 °C (c) and 550 °°C (d).

total elongation of EUROFER97-3_980/780 (Fig. 5a) is significantly greater than that of EUROFER97-3_1100/700 (Fig. 4a).

Fig. 7 summarizes the analysis of the stress–strain curves from Figs. 4 and 5, presenting the yield strength ($\sigma_{0.2}$), ultimate tensile strength (σ_B), and both uniform (ε_U) and total (ε_T) elongations for EUROFER97-3 before and after irradiation. Fig. 8a displays the processed data from Fig. 7a, illustrating the radiation-induced evolution of the yield strength $\sigma_{0.2}$, while Fig. 8b presents the processed data from Fig. 7c, showing the corresponding changes in the uniform elongation ε_U. Together, Fig. 8 highlights the radiation hardening and embrittlement effects in EUROFER97-3, expressed as the differences in $\sigma_{0.2}$ and ε_U values before and after irradiation. For clarity, the tensile test results at each testing temperature in Fig. 8 were averaged.

Summarizing the data shown in Figs. 4–8, we can highlight the features in the radiation-induced evolution of tensile properties of the EUROFER97-3 steel as follows.

In the unirradiated condition, the two heat treatments of EUROFER97-3 show clear differences in mechanical performance: EUROFER97-3_1100/700 exhibits higher strength but lower ductility, whereas EUROFER97-3_980/780 shows lower strength combined with higher ductility.

After irradiation at 330 °C, both heat-treated variants exhibit pronounced radiation hardening, reflected in a substantial increase in both yield and ultimate tensile strengths. At the same time, the uniform elongation decreases sharply to below 1 %, while the total elongation remains within the range of 2–10 %. The extent of radiation hardening—expressed as the increase in strength relative to the unirradiated state—is comparable for both heat treatments.

In contrast, irradiation at 540 °C results in only minor changes to the yield and ultimate strengths compared to the unirradiated condition. Likewise, neither the uniform nor the total elongation shows a noticeable degradation, remaining close to the baseline values.

In summary, the tensile test results for EUROFER97-3 subjected to two different heat treatments and irradiated to 20 dpa clearly demonstrate that irradiation temperature—330 °C versus 540 °C—has a fundamentally different impact on the mechanical behavior (see Fig. 8). At 330 °C, the tensile properties degrade severely due to strong radiation embrittlement, most evident from the drastic reduction in uniform elongation (Fig. 8b). Conversely, at 540 °C, detrimental effects are minimal: the steel largely preserves its plasticity and even shows a modest increase in strength (Fig. 8a), which can be considered a favorable outcome.

4. Discussion

Low-temperature radiation embrittlement of ferritic-martensitic steels is a well-known phenomenon, and it has also been extensively studied in EUROFER97 steel [12–16]. Reference [14] reports a sharp decrease in ductility following irradiation at 300–335 °C, as well as shows the dose dependence of radiation hardening in EUROFER97. From this dose dependence, it follows that a rapid increase in radiation hardening occurs at relatively low doses of up to 10 dpa [17–19]. Gaganidze [14] attributes radiation hardening primarily to the formation of radiation-induced defects such as dislocation loops. These defects act as obstacles to dislocation movement, leading to significant material hardening. The magnitude of radiation hardening is described by an

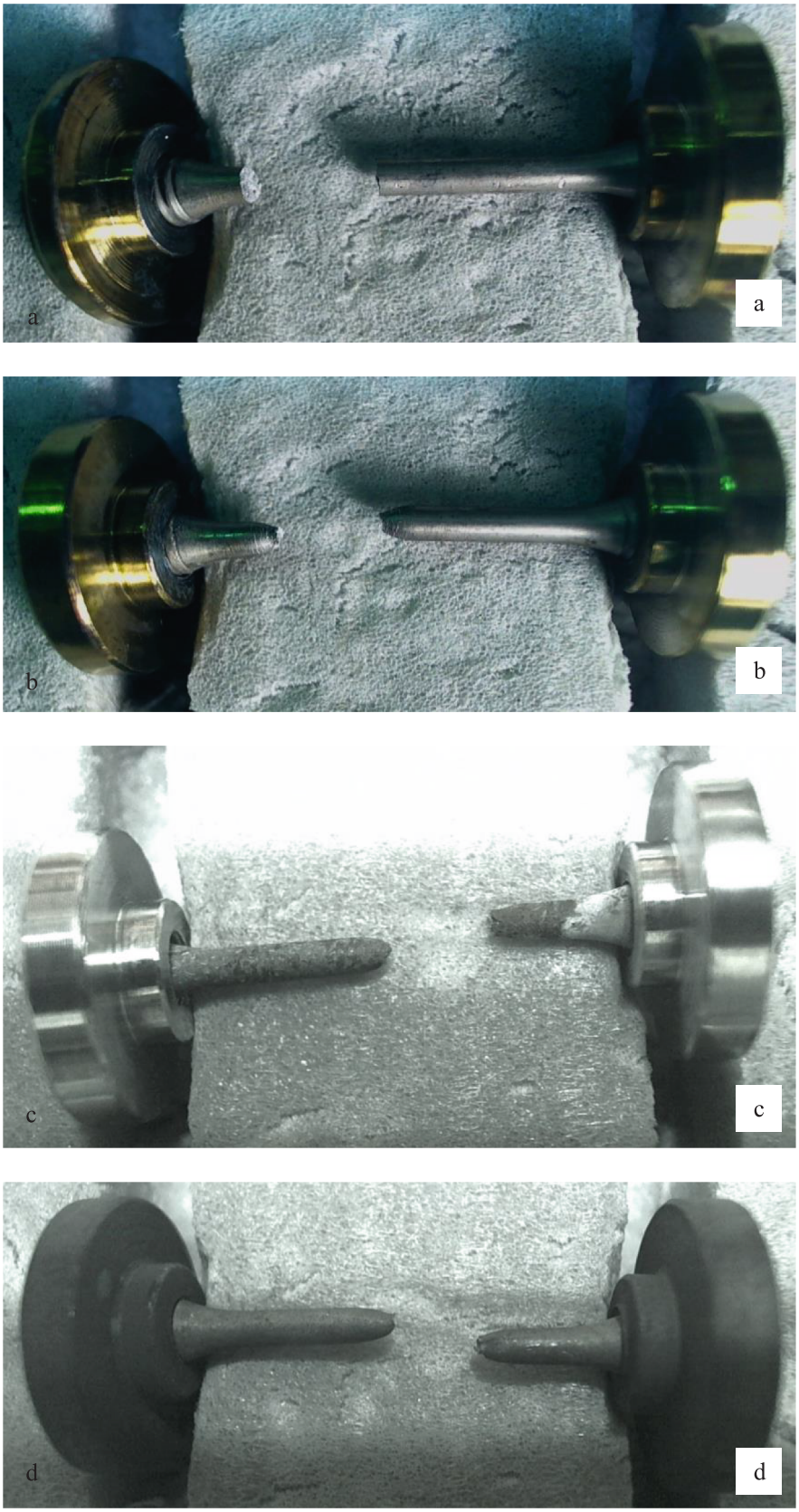

Fig. 6. Appearance of fragments of irradiated EUROFER97-3 specimens after tensile testing at T_{test} = 25 °C: a) 1100/700, T_{irr} = 330 °C; b) 980/780, T_{irr} = 330 °C; c) 1100/700, T_{irr} = 540 °C; d) 980/780, T_{irr} = 540 °C.

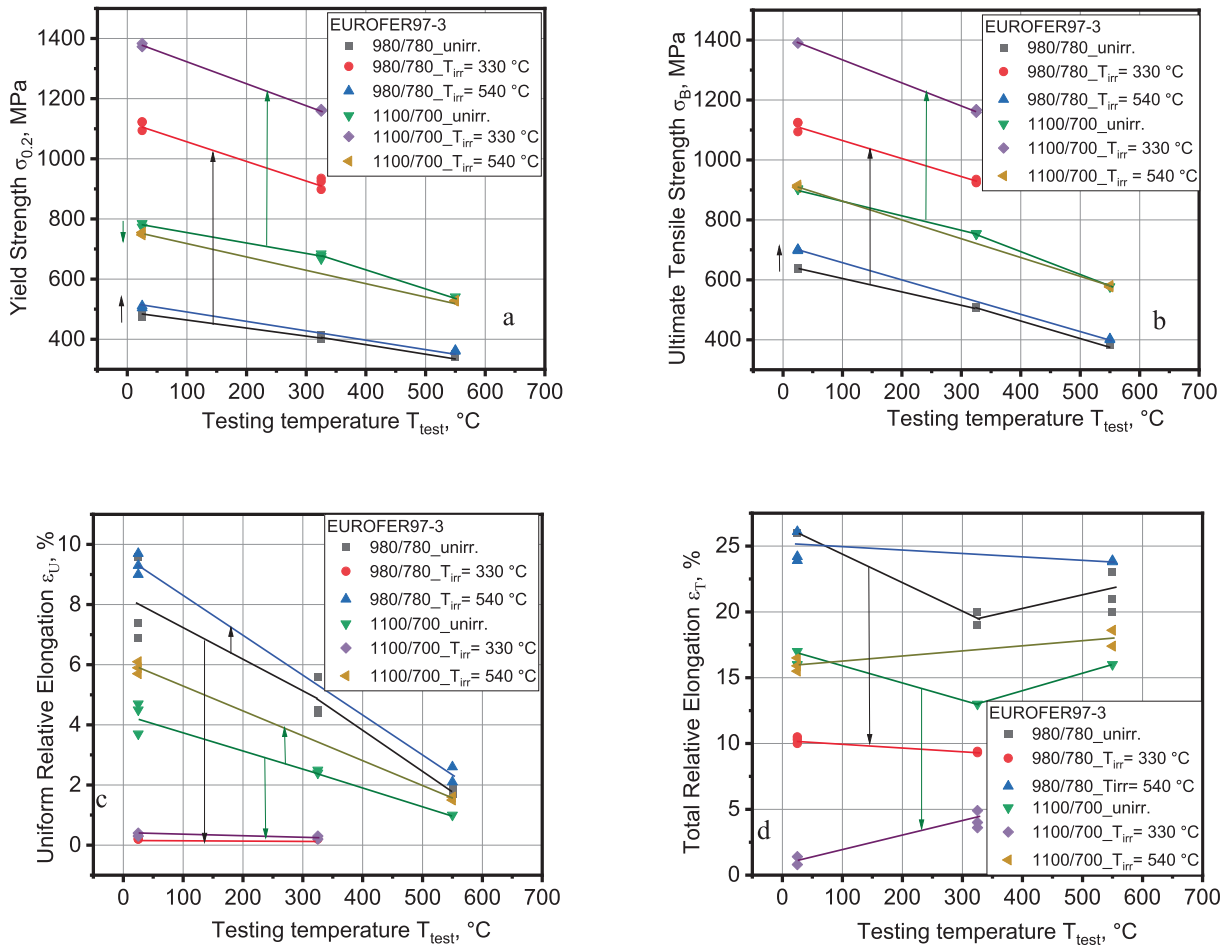

Fig. 7. Yield strength $\sigma_{0.2}$ (a), ultimate tensile strength σ_B (b), uniform relative elongation ε_U (c) and total relative elongation ε_T (d) of EUROFER97-3 before and after irradiation.

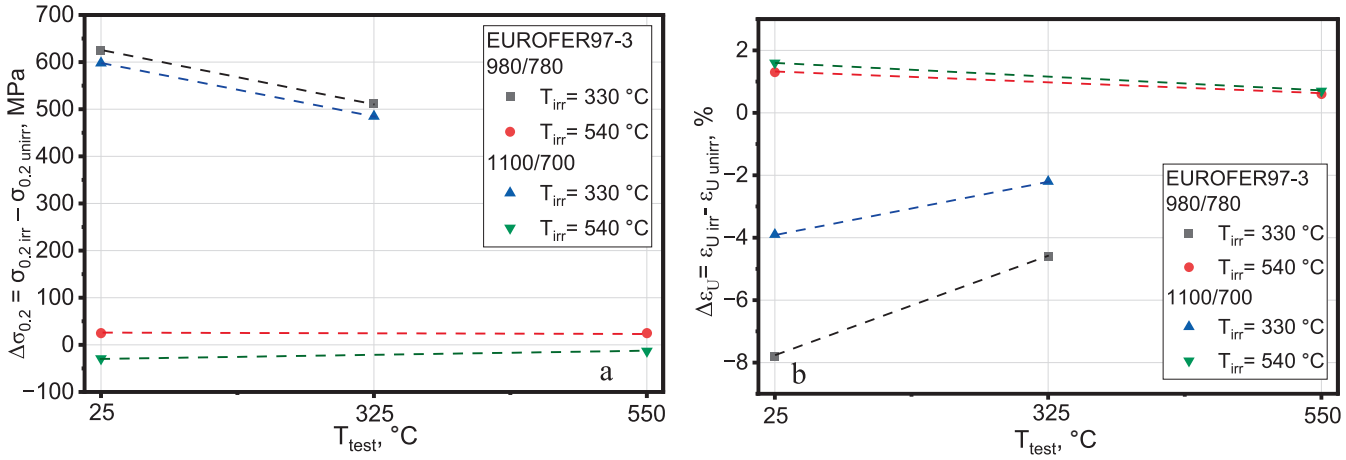

Fig. 8. Radiation-induced evolution of yield strength $\Delta\sigma_{0.2} = \sigma_{0.2irr} - \sigma_{0.2unirr}$ (radiation hardening) (a) and uniform relative elongation $\Delta\varepsilon_U = \varepsilon_{Uirr} - \varepsilon_{Uunirr}$ (radiation embrittlement) (b) of EUROFER97-3 where $\sigma_{0.2unirr}$ and $\sigma_{0.2irr}$ are the yield strength before and after irradiation, respectively, and ε_{Uunirr} and ε_{Uirr} are the uniform relative elongation before and after irradiation, respectively.

exponential dependence on damage dose, as expressed in equation (3) in [14].

Fig. 9 presents a fragment of the high-dose region of the diagram in Fig. 1 from [14], which also includes results from our study at the 20 dpa damage dose. A sharp increase in radiation hardening is observed as the dose increases from 16 to 20 dpa. However, further increase in the damage dose from 20 to 70 dpa does not lead to additional hardening, indicating the occurrence of a saturation within the 20–70 dpa dose range.

It should be noted that the heat treatment parameters do not fundamentally influence the magnitude of radiation hardening. Nonetheless, the radiation hardening was consistently slightly higher for heat

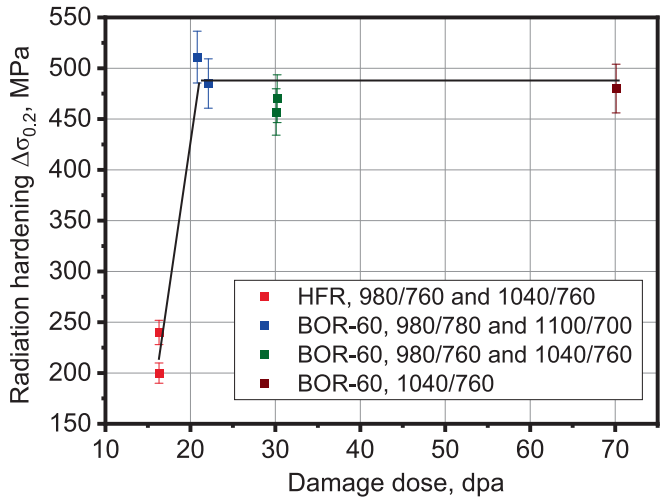

Fig. 9. Radiation hardening $\Delta\sigma_{0.2}$ vs. damage dose for EUROFER97 steel for T_{irr} = 325–350 °C and $T_{test} = T_{irr}$. There are two symbols for each dose, the one located higher corresponds always to second heat treatment shown.

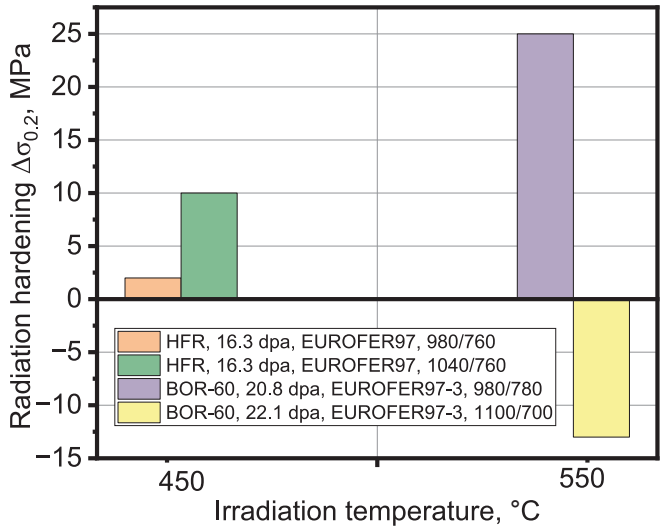

Fig. 10. Radiation hardening $\Delta\sigma_{0.2}$ vs. irradiation temperature for EUROFER97 steel T_{irr} = 450 and 540 °C and $T_{test} = T_{irr}$.

treatments involving a higher quenching temperature and a lower tempering temperature. This indirect evidence suggests that the primary mechanism behind radiation hardening and embrittlement of EUROFER97-3 steel is the formation of radiation-induced defects (such as dislocation loops), rather than microstructural changes in the original phase of this steel.

Fig. 10 illustrates the dependence of radiation hardening ($\Delta\sigma_{0.2}$) of EUROFER97 on irradiation temperature. There is very limited literature data on the tensile properties of EUROFER97 after neutron irradiation at relatively high temperatures above 400 °C. When irradiated at 450 °C, the radiation hardening is minimal [20]. As this study shows, irradiation at 540 °C results in either negligible hardening or even softening, depending on the heat treatment. This indicates that at irradiation temperatures exceeding 400 °C, the effects of annealing radiation-induced defects become dominant, significantly reducing their influence on the magnitude of radiation hardening and embrittlement.

Radiation-induced changes in the tensile properties of EUROFER97 under neutron irradiation occur due to the formation of radiation defects and possible evolution of the original microstructure. Currently, no experimental data is available regarding the microstructural evolution of EUROFER97 at irradiation temperatures above 450 °C. Klimenkov [21–25] studied the microstructure of EUROFER97 and EUROFER97-ODS steels after irradiation at 300–450 °C to a dose of 16.3 dpa (in the HFR), observing the formation of "black dots" and dislocation loops (in steels without boron additives). Gaganidze [14] performed TEM analyses of EUROFER97 irradiated at 332 °C to 32 dpa in the BOR-60 fast reactor and observed the formation of dislocation loops.

Dvoriashin [26] investigated EP450, a Russian ferritic/martensitic steel containing 11–13.5 wt% Cr, after irradiation in the BR-10 research reactor and BN-350 and BN-600 fast reactors at temperatures of 275–690 °C to doses of 0.5–89 dpa. He observed the formation of voids, dislocation loops, and new precipitates compared to the unirradiated microstructure, with their sizes and concentrations depending on irradiation conditions. Voids were observed at almost all parameters but were absent after irradiation at 360 °C to 9.7 dpa, 595 °C to 39 dpa, and 690 °C to 17 dpa. Between 275 °C and 520 °C, a high density of fine precipitates was found in both ferrite and tempered martensite phases. These precipitates included the α-phase (ferrite enriched with chromium). The χ-phase appeared at 460–590 °C, with particle sizes ranging from 35 to 60 nm as temperature increased. Rod-like M_2X particles were formed in the 460–690 °C range, with sizes increasing from 80 to 600 nm. Irradiation at 510–690 °C caused growth of $M_{23}C_6$ carbides along grain boundaries.

TEM analysis of the specimens from this study, irradiated at 330 °C and 540 °C to 20 dpa, is scheduled to commence in 2026. This will help clarify the radiation-induced microstructural parameters of EUROFER97-3 and more definitively link microstructural evolution to the changes in tensile properties.

5. Conclusions

The tensile properties of EUROFER97-3 steel were investigated on specimens subjected to two heat treatments (EUROFER97-3_1100/700 and EUROFER97-3_980/780) after irradiation in the BOR-60 fast reactor at target temperatures of 325 ± 10 °C and 550 ± 20 °C (with actual average temperatures of 330 °C and 540 °C, respectively). The irradiation damage doses ranged from 19.2 to 23.3 dpa.

The main findings of this study are as follows:

- At 330 °C, irradiation produces pronounced radiation hardening, characterized by a marked increase in both yield strength and ultimate tensile strengths, accompanied by a sharp reduction in uniform elongation to less than 1 %. Nevertheless, the total elongation remains within 2–10 %. These results are consistent with literature data, confirming that radiation hardening saturates in the dose range of 20–70 dpa.
- At 540 °C, irradiation causes only minor changes in both yield and ultimate tensile strengths, and both uniform and total relative elongations compared with unirradiated reference data. These findings—obtained for the first time on radiation hardening and embrittlement of EUROFER97 steel irradiated at a relatively high temperature of 540 °C, —demonstrate the absence of critical changes in the strength and ductility. In fact, the tensile properties of the irradiated steel are essentially indistinguishable from those in the unirradiated reference state.
- This fundamental difference in the irradiation response between 330 °C and 540 °C can be attributed to the formation of radiation-induced defects (black dots, dislocation loops, voids), the precipitation of new fine radiation-induced phases, and the microstructural evolution of the original phase structure. These phenomena will be further investigated through subsequent TEM analysis of the irradiated EUROFER97-3 specimens.

CRediT authorship contribution statement

Vladimir Chakin: Writing – review & editing, Writing – original

draft, Supervision, Methodology, Investigation, Formal analysis, Conceptualization. **Carsten Bonnekoh:** Writing – review & editing, Methodology, Investigation, Formal analysis. **Ramil Gaisin:** Writing – review & editing, Investigation, Formal analysis, Data curation. **Rainer Ziegler:** Writing – review & editing, Investigation, Conceptualization. **Michael Duerrschnabel:** Writing – review & editing, Validation, Software, Formal analysis, Data curation. **Michael Klimenkov:** Writing – review & editing, Investigation, Formal analysis. **Bronislava Gorr:** Writing – review & editing, Resources, Methodology, Funding acquisition, Conceptualization. **Michael Rieth:** Writing – review & editing, Supervision, Project administration, Methodology, Formal analysis, Data curation, Conceptualization.

Declaration of competing interest

The authors declare that they have no known competing financial interests or personal relationships that could have appeared to influence the work reported in this paper.

Acknowledgements

This work has been carried out within the framework of the EUROfusion Consortium, funded by the European Union via the Euratom Research and Training Programme (Grant Agreement No 101052200 — EUROfusion). Views and opinions expressed are, however, those of the authors only and do not necessarily reflect those of the European Union or the European Commission. Neither the European Union nor the European Commission can be held responsible for them.

We would like to express our sincere gratitude to the staff of the Research Institute of Atomic Reactors for their organization of the irradiation and post-irradiation examinations of the materials, as well as for the insightful and fruitful discussions regarding the results obtained in this study.

We also thank Dr. Thomas Bergfeldt for the chemical analysis of the EUROFER97-3 steel, Daniel Bolich for performing heat treatments and preparation of the specimens for microstructure studies, Leyla Franz for performing of microhardness measurements and excellent assistance in preparing the paper materials.

Data availability

No data was used for the research described in the article.

References

[1] M. Rieth, M. Dürrschnabel, S. Bonk, U. Jäntsch, T. Bergfeldt, J. Hoffmann, S. Antusch, E. Simondon, M. Klimenkov, C. Bonnekoh, B.-E. Ghidersa, H. Neuberger, J. Rey, C. Zeile, G. Pintsuk, G. Aiello, Technological Processes for Steel applications in Nuclear Fusion, Appl. Sci. 11 (2021) 11653, https://doi.org/10.3390/app112411653.

[2] M. Rieth, M. Dürrschnabel, S. Bonk, S. Antusch, G. Pintsuk, G. Aiello, J. Henry, Y. de Carlan, B.-E. Ghidersa, H. Neuberger, et al., Fabrication routes for advanced first wall design alternatives, Nucl. Fusion 61 (2021) 116067.

[3] G. Federici, C. Bachmann, L. Barucca, W. Biel, L. Boccaccini, R. Brown, C. Bustreo, S. Ciattaglia, F. Cismondi, M. Coleman, V. Corato, C. Day, E. Diegele, U. Fischer, T. Franke, C. Gliss, A. Ibarra, R. Kembleton, A. Loving, F. Maviglia, B. Meszaros, G. Pintsuk, N. Taylor, M.Q. Tran, C. Vorpahl, R. Wenninger, J.H. You, DEMO design activity in Europe: Progress and updates, Fusion Eng. Des. 136 (2018) 729–741.

[4] G. Federici, L. Boccaccini, F. Cismondi, M. Gasparotto, Y. Poitevin, I. Ricapito, An overview of the EU breeding blanket design strategy as an integral part of the DEMO design effort, Fusion Eng. Des. 141 (2019) 30–42.

[5] F.A. Hernández, P. Pereslavtsev, G. Zhou, Q. Kang, S. D'Amico, H. Neuberger, L. V. Boccaccini, B. Kiss, G. Nádasi, L. Maqueda, I. Cristescu, I. Moscato, I. Ricapito, F. Cismondi, Consolidated design of the HCPB Breeding Blanket for the pre-Conceptual Design phase of the EU DEMO and harmonization with the ITER HCPB TBM program, Fusion Eng. Des. 157 (2020) 111614.

[6] M. Duerrschnabel, U. Jaentsch, R. Gaisin, M. Rieth, Microstructural insights into EUROFER97 batch 3 steels, Nucl. Mater. Energy 35 (2023) 101445.

[7] A.L. Izhutov, Y.M. Krasheninnikov, I.Y. Zhemkov, A.V. Varivtsev, Y. V. Naboischikov, V.S. Neustroev, V.K. Shamardin, Prolongation of the BOR-60 reactor operation, Nucl. Eng. Techn. 47 (3) (2015) 253–259.

[8] V. Chakin, C. Bonnekoh, R. Ziegler, R. Gaisin, M. Duerrschnabel, M. Klimenkov, M. Rieth, B. Gorr, M. Toloczko, Creep behavior of EUROFER97–3 steel during neutron irradiation at 325 °C and 550 °C to 7–24 dpa, Fusion Eng. Des. 215 (2025) 115014.

[9] V. Chakin, R. Gaisin, C. Bonnekoh, M. Duerrschnabel, M. Rieth, B. Gorr, M. Brodnikikovsky, M. Krapivka, S. Firstov, Embrittlement of chromium alloys after neutron irradiation at high temperatures to damage doses of 10–46 dpa, Nucl. Mater. Energy 42 (2025) 101871.

[10] L.V. Gorynin, V.A. Ignatov, V.V. Rybin, S.A. Fabritsiev, V.A. Kazakov, V.P. Chakin, V.A. Tsykanov, V.R. Barabash, Y.G. Prokofyev, Effects of neutron irradiation on properties of refractory metals, J. Nucl. Mater. 191–194 (1992) 421–425.

[11] R.G. Abernethy, J.-S.-K.-L. Gibson, A. Giannattasio, J.D. Murphy, O. Wouters, S. Bradnam, L.W. Packer, M.R. Gilbert, M. Klimenkov, M. Rieth, H.-C. Schneider, C. D. Hardie, S.G. Roberts, D.E.J. Armstrong, Effects of neutron irradiation on the brittle to ductile transition in single crystal tungsten, J. Nucl. Mater. 527 (2019) 151799.

[12] C. Petersen, A. Povstyanko, V. Prokhorov, A. Fedoseev, O. Makarov, M. Walter, Tensile and low cycle fatigue properties of different ferritic/martensitic steels after the fast reactor irradiation 'ARBOR 1', J. Nucl. Mater. 386–388 (2009) 299–302.

[13] C. Cabet, F. Dalle, E. Gaganidze, J. Henry, H. Tanigawa, Ferritic-martensitic steels for fission and fusion applications, J. Nucl. Mater. 523 (2019) 510–537.

[14] E. Gaganidze, C. Petersen, E. Materna-Morris, C. Dethloff, O.J. Weiß, J. Aktaa, A. Povstyanko, A. Fedoseev, O. Makarov, V. Prokhorov, Mechanical properties and TEM examination of RAFM steels irradiated up to 70 dpa in BOR-60, J. Nucl. Mater. 417 (2011) 93–98.

[15] C. Bob van der Schaaf, Y.D. Petersen, J.W. Carlan, E. Rensman, X.A. Gaganidze, High dose, up to 80 dpa, mechanical properties of Eurofer 97, J. Nucl. Mater. 386–388 (2009) 236–240.

[16] O. Kachko, A. Puype, D. Terentyev, C.-C. Chang, M. Rieth, R.H. Petrov, Impact of neutron irradiation on the tensile properties of advanced EUROFER97-type steels, J. Nucl. Mater. 599 (2024) 155176.

[17] A. Alamo, J.L. Bertin, V.K. Shamardin, P. Wident, J. Nucl. Mater. 367–370 (2007) 54–59.

[18] E. Lucon, R. Chaouadi, M. Decreton, et al., J. Nucl. Mater. 329–333 (2004) 1078–1082.

[19] J. Rensman, N.R.G. Irradiation Testing, Report on 300 °C and 60 °C Irradiated RAFM Steels, Petten (2005), 20023/05.68497/P.

[20] E. Materna-Morris, A. Möslang, R. Rolli, H.-C. Schneider, J. Nucl. Mater. 386–388 (2009) 422–425.

[21] M. Klimenkov, U. Jeantsch, M. Rieth, A. Moeslang, Correlation of microstructural and mechanical properties of neutron irradiated EUROFER97 steel, J. Nucl. Mater. 538 (2020) 152231.

[22] M. Klimenkov, U. Jäntsch, M. Rieth, M. Dürrschnabel, A. Möslang, H.C. Schneider, Post-irradiation microstructural examination of EUROFER-ODS steel irradiated at 300 °C and 400 °C, J. Nucl. Mater. 557 (2021) 153259.

[23] M. Klimenkov, A. Möslang, E. Materna-Morris, Helium influence on the microstructure and swelling of 9%Cr ferritic steel after neutron irradiation to 16.3 dpa, J. Nucl. Mater. 453 (2014) 54–59.

[24] R. Coppola, M. Klimenkov, A. Möslang, R. Lindau, M. Rieth, M. Valli, Microstructural effects of irradiation temperature and helium content in neutron irradiated B-alloyed Eurofer97-1 steel, Nucl. Mater. Energy 17 (2018) 40–47.

[25] M. Klimenkov, R. Lindau, E. Materna-Morris, A. Möslang, TEM characterization of precipitates in EUROFER 97, Prog. Nucl. Energy 57 (2012) 8–13.

[26] A.M. Dvoriashin, S.I. Porollo, Y.V. Konobeev, F.A. Garner, Influence of high dose neutron irradiation on microstructure of EP-450 ferritic–martensitic steel irradiated in three Russian fast reactors, J. Nucl. Mater. 329–333 (2004) 319–323.